Global Journal of Researches in Engineering: F
Electrical and Electronics Engineering
Volume 21 Issue 2 Version 1.0 Year 2021
Type: Double Blind Peer Reviewed International Research Journal
Publisher: Global Journals
Online ISSN: 2249-4596 & Print ISSN: 0975-5861

A Novel Approach for the Characterization of Triangular Modulated Frequency Modulated Continuous Wave Low Probability of Intercept Radar Signals via Application of the Wigner-Ville Distribution and the Reassigned Smoothed Pseudo Wigner-Ville Distribution

By Daniel L. Stevens

Abstract- Digital intercept receivers are changing from Fourier-based analysis to classical time-frequency analysis techniques for analyzing low probability of intercept radar signals. This paper presents a novel approach of characterizing low probability of intercept triangular modulated frequency modulated continuous wave radar signals through utilization and direct comparison of the signal processing techniques Wigner-Ville Distribution versus the Reassigned Smooth Pseudo Wigner-Ville Distribution. The following metrics were used for evaluation: percent error of: carrier frequency, modulation bandwidth, modulation period, chirp rate, and time-frequency localization (x and y direction). Also used were: percent detection, lowest signal-to-noise ratio for signal detection, and plot (processing) time. Experimental results demonstrate that overall, the Reassigned Smooth Pseudo Wigner-Ville Distribution signal processing technique produced more accurate characterization metrics than the Wigner-Ville Distribution signal processing technique.

An improvement in performance may equate to an increase in personnel safety.

GJRE-F Classification: *FOR Code: 290901*

ANOVELAPPROACHFORTHECHARACTERIZATIONOFTRIANGULARMODULATEDFREQUENCYMODULATEDCONTINUOUSWAVELOWPROBABILITYOFINTERCEPTRADARSIGNALSVIAAPPLICATIONOFTHEWIGNERVILLEDISTRIBUTI
ONANDTHEREASSIGNEDSMOOTHEDPSEUDOWIGNERVILLEDISTRIBUTION

Strictly as per the compliance and regulations of:

A Novel Approach for the Characterization of Triangular Modulated Frequency Modulated Continuous Wave Low Probability of Intercept Radar Signals via Application of the Wigner-Ville Distribution and the Reassigned Smoothed Pseudo Wigner-Ville Distribution[1]

Daniel L. Stevens

Abstract- Digital intercept receivers are changing from Fourier-based analysis to classical time-frequency analysis techniques for analyzing low probability of intercept radar signals. This paper presents a novel approach of characterizing low probability of intercept triangular modulated frequency modulated continuous wave radar signals through utilization and direct comparison of the signal processing techniques Wigner-Ville Distribution versus the Reassigned Smooth Pseudo Wigner-Ville Distribution. The following metrics were used for evaluation: percent error of: carrier frequency, modulation bandwidth, modulation period, chirp rate, and time-frequency localization (x and y direction). Also used were: percent detection, lowest signal-to-noise ratio for signal detection, and plot (processing) time. Experimental results demonstrate that overall, the Reassigned Smooth Pseudo Wigner-Ville Distribution signal processing technique produced more accurate characterization metrics than the Wigner-Ville Distribution signal processing technique.

An improvement in performance may equate to an increase in personnel safety.

I. Introduction

The Low Probability of Intercept (LPI) signal used for this paper is the Frequency Modulated Continuous Wave (FMCW) signal, which is commonly used in modern radar systems [WAN10], [WON09], [WAJ08]. The frequency modulation spreads the transmitted energy over a large modulation bandwidth ΔF, providing good range resolution that is essential for discriminating targets from clutter. The power spectrum of the FMCW signal is nearly rectangular over the modulation bandwidth, so non-cooperative interception can be challenging. Since the transmit waveform is deterministic, the form of the return signals can be predicted. This gives it the added advantage of being resistant to interference (such as jamming), since any signal not matching this form can be suppressed [WIL06]. Consequently, it is problematic for an intercept receiver to detect the FMCW waveform and measure the parameters accurately enough to match the jammer waveform to the radar waveform [PAC09].

The most prevalent linear modulation utilized is the triangular FMCW emitter [LIA09], since it can measure the target's range and Doppler [MIL02], [LIW08]. Triangular modulated FMCW is the waveform that is employed for this paper.

Time-frequency signal analysis involves the analysis and processing of signals with time-varying frequency content. These signals are best represented by a time-frequency distribution [PAP95], [HAN00], which shows how the energy of the signal is distributed over the two-dimensional time-frequency plane [WEI03], [LIX08], [OZD03]. Processing of the signal can exploit the features produced by the concentration of signal energy in two dimensions (time and frequency), instead of in one dimension (time or frequency) [BOA03], [LIY03]. Noise tends to spread out evenly over the time-frequency domain, whereas signals concentrate their energies within limited time intervals and frequency bands; therefore the local SNR of a 'noisy' signal can be improved simply by using time-frequency analysis [XIA99]. In addition, the intercept receiver can increase its processing gain simply by implementing time-frequency signal analysis [GUL08].

Time-frequency representations are valuable for the visual interpretation of signal dynamics [RAN01]. An experienced operator can more easily detect a signal and extract the signal parameters by analyzing a time-frequency representation, vice a time representation, or a frequency representation [ANJ09].

One of the members of the time-frequency analysis techniques family is the Wigner-Ville Distribution (WVD). The WVD has a number of desirable

Author: Air Force Research Laboratory, Rome, NY 13441.
e-mail: daniel.stevens.7@us.af.mil

[1] Approved for Public Release; Distribution Unlimited: Case Number: AFRL-2021-1236 20210421

mathematical properties: it is always real-valued, it preserves time and frequency shifts, and it satisfies marginal properties [QIA02]. The WVD is computed by correlating the signal with a time and frequency translated version of itself, making it bilinear. The WVD has the highest signal energy concentration in the time-frequency plane [WIL06]. By using the WVD, an intercept receiver can come close to having a processing gain near the LPI radar's matched filter processing gain [PAC09]. The WVD, however, contains cross term interference between each pair of signal components, which may limit its applications [GUL07], [STE96], and which can make the WVD time-frequency representation hard to read, especially if the components are numerous or close to each other, and the more so in the presence of noise [BOA03]. This lack of readability may equate to less accurate signal detection and parameter extraction metrics, potentially placing the intercept receiver signal analyst's platform in harm's way.

The WVD of a signal x(t) is given in equation (1) as:

$$W_x(t,f) = \int_{-\infty}^{+\infty} x(t+\frac{\tau}{2})x^*\left(t-\frac{\tau}{2}\right)e^{-j2\pi f\tau}\,d\tau \qquad (1)$$

or equivalently in equation (2) as:

$$W_x(t,f) = \int_{-\infty}^{+\infty} X(f+\frac{\xi}{2})X^*\left(f-\frac{\xi}{2}\right)e^{j2\pi\xi t}\,d\xi \qquad (2)$$

A lack of readability must be overcome in order to obtain time-frequency distributions that can be easily read by operators and easily included in a signal processing application [BOA03].

Some efforts have been made recently in that direction, and in particular, a general methodology referred to as reassignment.

The original idea of reassignment was introduced in an attempt to improve the Spectrogram [OZD03]. As with any other bilinear energy distribution, the Spectrogram is faced with an unavoidable trade-off between the reduction of misleading interference terms and a sharp localization of the signal components.

We can define the Spectrogram as a two-dimensional convolution of the WVD of the signal by the WVD of the analysis window, as in equation (3):

$$S_x(t,f;h) = \iint_{-\infty}^{+\infty} W_x(s,\xi)W_h(t-s,f-\xi)ds\,d\xi \qquad (3)$$

Therefore, the distribution reduces the interference terms of the signal's WVD, but at the expense of time and frequency localization. However, a closer look at equation (3) shows that $W_h(t-s,f-\xi)$ delimits a time-frequency domain at the vicinity of the (t,f) point, inside which a weighted average of the signal's WVD values is performed. The key point of the reassignment principle is that these values have no reason to be symmetrically distributed around (t,f), which is the geometrical center of this domain. Therefore, their average should not be assigned at this point, but rather at the center of gravity of this domain, which is much more representative of the local energy distribution of the signal [AUG94]. Reasoning with a mechanical analogy, the local energy distribution $W_h(t-s,f-\xi)W_x(s,\xi)$ (as a function of s and ξ) can be considered as a mass distribution, and it is much more accurate to assign the total mass (i.e. the Spectrogram value) to the center of gravity of the domain rather than to its geometrical center. Another way to look at it is this: the total mass of an object is assigned to its geometrical center, an arbitrary point which except in the very specific case of a homogeneous distribution, has no reason to suit the actual distribution. A much more meaningful choice is to assign the total mass of an object, as well as the Spectrogram value, to the center of gravity of their respective distribution [BOA03].

This is precisely how the reassignment method proceeds: it moves each value of the Spectrogram computed at any point (t,f) to another point $(\hat{t},\hat{f})$ which is the center of gravity of the signal energy distribution around (t,f) (see equations (4) and (5)) [LIX08]:

$$\hat{t}(x;t,f) = \frac{\iint_{-\infty}^{+\infty} s\,W_h(t-s,f-\xi)W_x(s,\xi)ds\,d\xi}{\iint_{-\infty}^{+\infty} W_h(t-s,f-\xi)W_x(s,\xi)ds\,d\xi} \qquad (4)$$

$$\hat{f}(x;t,f) = \frac{\iint_{-\infty}^{+\infty} \xi\,W_h(t-s,f-\xi)W_x(s,\xi)ds\,d\xi}{\iint_{-\infty}^{+\infty} W_h(t-s,f-\xi)W_x(s,\xi)ds\,d\xi} \qquad (5)$$

And thus leads to a reassigned Spectrogram (equation (6)), whose value at any point (t',f') is the sum of all the Spectrogram values reassigned to this point:

$$S_x^{(r)}(t',f';h) = \iint_{-\infty}^{+\infty} S_x(t,f;h)\delta\big(t'-\hat{t}(x;t,f)\big)\delta\Big(f'-\hat{f}(x;t,f)\Big)\,dt\,df \qquad (6)$$

One of the most interesting properties of this new distribution is that it also uses the phase information of the STFT, and not only its squared modulus as in the Spectrogram. It uses this information from the phase spectrum to sharpen the amplitude estimates in time and frequency. This can be seen from the following expressions of the reassignment operators:

$$\hat{t}(x;t,f) = -\frac{d\Phi_x(t,f;h)}{df} \qquad (7)$$

$$\hat{f}(x;t,f) = f + \frac{d\Phi_x(t,f;h)}{dt} \qquad (8)$$

where $\Phi_x(t,f;h)$ is the phase of the STFT of x : $\Phi_x(t,f;h) = \arg(F_x$ (t, f; h)). However, these expressions (equations (7) and (8)) do not lead to an

efficient implementation, and have to be replaced by equations (9) (local group delay) and (10) (local instantaneous frequency):

$$\hat{t}(x;t,f) = t - \Re\left\{\frac{F_x(t,f;T_h)F_x^*(t,f;h)}{\left|F_{x(t,f;h)}\right|^2}\right\} \quad (9)$$

$$\hat{f}(x;t,f) = f - \Im\left\{\frac{F_x(t,f;D_h)F_x^*(t,f;h)}{\left|F_{x(t,f;h)}\right|^2}\right\} \quad (10)$$

Where $T_h(t) = t \times h(t)$ and $D_h(t) = \frac{dh}{dt}(t)$. This leads to an efficient implementation for the Reassigned Spectrogram without explicitly computing the partial derivatives of phase. The Reassigned Spectrogram may thus be computed by using 3 STFTs, each having a different window (the window function h; the same window with a weighted time ramp t*h; the derivative of the window function h with respect to time (dh/dt)). Reassigned Spectrograms are therefore very computationally efficient to implement.

Since time-frequency reassignment is not a bilinear operation, it does not permit a stable reconstruction of the signal. In addition, once the phase information has been used to reassign the amplitude coefficients, it is no longer available for use in reconstruction. For this reason, the reassignment method has received limited attention from engineers, and its greatest potential seems to be where reconstruction is not necessary, that is, where signal analysis is an end unto itself.

One of the most important properties of the reassignment method is that the application of the reassignment process to any distribution of Cohen's class theoretically yields perfectly localized distributions for chirp signals, frequency tones, and impulses. This is one of the reasons that the reassignment method was chosen for this paper as a signal processing technique for analyzing LPI radar waveforms such as the triangular modulated FMCW waveforms (which can be viewed as back-to-back chirps).

In order to rectify the classical time-frequency analysis deficiency of cross-term interference, a method needs to be utilized that reduces cross-terms, which the reassignment method does.

The reassignment principle for the Spectrogram allows for a straight-forward extension of its use for other distributions as well [HIP00], including the WVD. If we consider the general expression of a distribution of the Cohen's class as a two-dimensional convolution of the WVD, as in equation (11):

$$C_x(t,f;\Pi) = \iint_{-\infty}^{+\infty} \Pi(t-s,f-\xi)W_x(s,\xi)ds\,d\xi \quad (11)$$

Replacing the particular smoothing kernel $W_h(u,\xi)$ by an arbitrary kernel $\Pi(s,\xi)$ simply defines the reassignment of any member of Cohen's class (equations (12) through (14)):

$$\hat{t}(x;t,f) = \frac{\iint_{-\infty}^{+\infty} s\,\Pi(t-s,f-\xi)W_x(s,\xi)ds\,d\xi}{\iint_{-\infty}^{+\infty} \Pi(t-s,f-\xi)W_x(s,\xi)ds\,d\xi} \quad (12)$$

$$\hat{f}(x;t,f) = \frac{\iint_{-\infty}^{+\infty} \xi\,\Pi(t-s,f-\xi)W_x(s,\xi)ds\,d\xi}{\iint_{-\infty}^{+\infty} \Pi(t-s,f-\xi)W_x(s,\xi)ds\,d\xi} \quad (13)$$

$$C_x^{(r)}(t',f';\Pi) = \iint_{-\infty}^{+\infty} C_x(t,f;\Pi)\delta\left(t' - \hat{t}(x;t,f)\right)\delta\left(f' - \hat{f}(x;t,f)\right)dt\,df \quad (14)$$

The resulting reassigned distributions (which includes the RSPWVD) efficiently produce a reduction of the interference terms provided by a well adapted smoothing kernel. In addition, the reassignment operators $\hat{t}(x;t,f)$ and $\hat{f}(x;t,f)$ are very computationally efficient [AUG95].

II. Methodology

The methodologies detailed in this section describe the processes involved in obtaining and comparing metrics between the WVD signal processing technique and the RSPWVD signal processing technique for the detection and characterization of low probability of intercept triangular modulated FMCW radar signals.

The tools used for this testing were: MATLAB (version 8.3), Signal Processing Toolbox (version 6.21), and Time-Frequency Toolbox (version 1.0) (http://tftb.nongnu.org/).

All testing was accomplished on a desktop computer (Dell Precision T1700; Processor -Intel Xeon CPU E3-1226 v3 3.30GHz; Installed RAM - 32.0GB; System type - 64-bit operating system, x64-based processor).

Testing was performed for the triangular modulated FMCW waveform, whose parameters were chosen for academic validation of signal processing techniques. Due to computer processing resources they were not meant to represent real-world values. The number of samples was chosen to be 256, which seemed to be optimum size for the desktop computer. Testing was performed at three different SNR levels: 10dB, 0dB, and the lowest SNR at which the signal could be detected. The noise added was white Gaussian noise, which best reflects the thermal noise present in the IF section of an intercept receiver [PAC09]. Kaiser windowing was used, where windowing was applicable. 250 runs were performed for each test, for statistical purposes. The plots included in this paper were done at a threshold of 5% of the maximum intensity and were linear scale (not dB) of analytic (complex) signals; the color bar represented intensity.

The signal processing techniques used for each task were the WVD and the RSPWVD.

The triangular modulated FMCW signal (most prevalent LPI radar waveform [LIA09]) used had the following parameters: sampling frequency=4KHz; carrier frequency=1KHz; modulation bandwidth= 500Hz; modulation period=.02sec.

After each individual run for each individual test, metrics were extracted from the time-frequency representation. The metrics that were extracted were as follows:

Relative processing time: The relative processing time for each time-frequency representation.

Percent detection: Percent of time signal was detected - signal was declared a detection if any portion of each of the signal components (4 chirp components for triangular modulated FMCW) exceeded a set threshold (a certain percentage of the maximum intensity of the time-frequency representation).

Threshold percentages were determined based on visual detections of low SNR signals (lowest SNR at which the signal could be visually detected in the time-frequency representation) (see Figure 1).

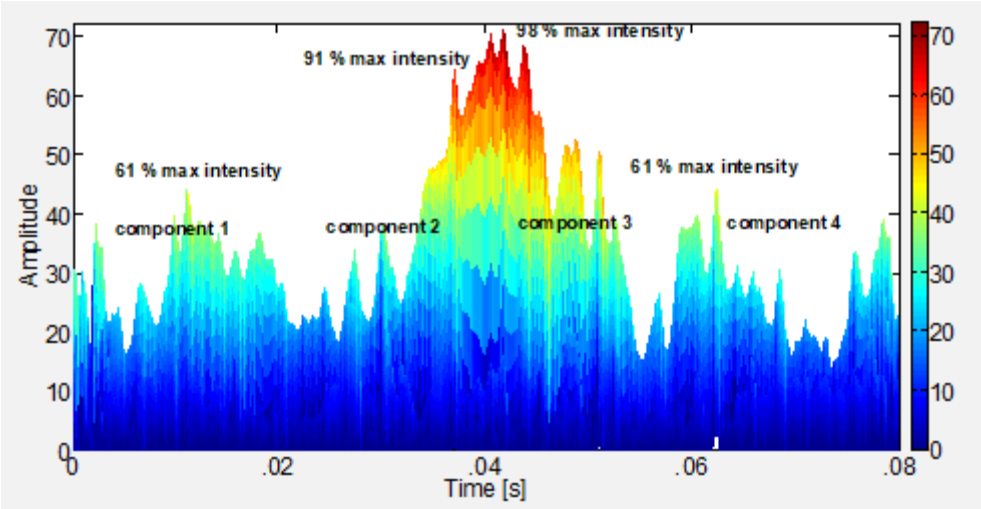

Figure 1: Threshold percentage determination. This plot is a time vs. amplitude (x-z view) of a signal processing technique of a triangular modulated FMCW signal (256 samples, with SNR= -3dB). For visually detected low SNR plots (like this one), the percent of max intensity for the peak z-value of each of the signal components (the 2 legs for each of the 2 triangles of the triangular modulated FMCW) was noted (here 61%, 91%, 98%, 61%), and the lowest of these 4 values was recorded (61%). Ten test runs were performed for this waveform for each of the signal processing techniques that were used. The average of these recorded low values was determined and then assigned as the threshold for that particular signal processing technique.

Based on the above methodology, thresholds were assigned as follows for the signal processing techniques used for this paper: WVD (50%); RSPWVD (50%)

For percent detection determination, these threshold values were included for each of the signal processing technique algorithms so that the thresholds could be applied automatically during the plotting process. From the time-frequency representation threshold plot, the signal was declared a detection if any portion of each of the signal components was visible (see Figure 2).

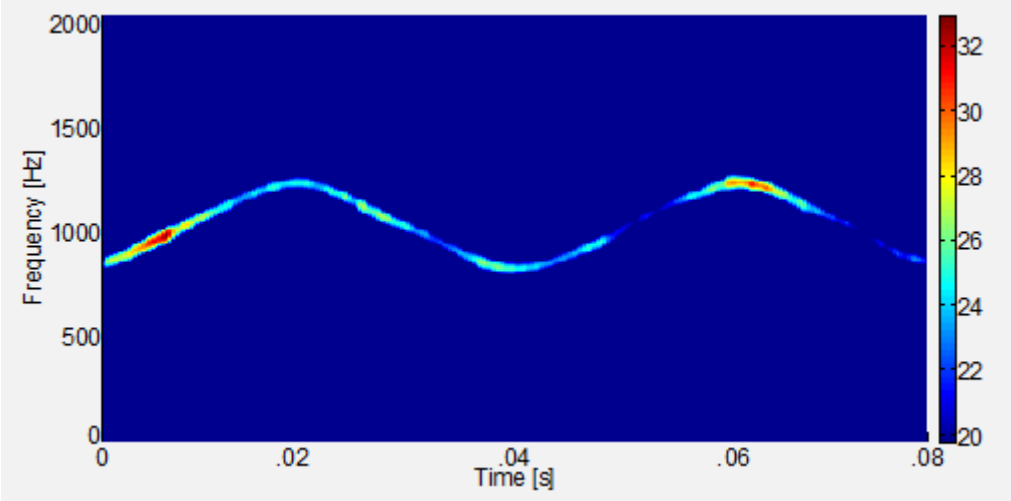

Figure 2: Percent detection (time-frequency). This plot is a time vs. frequency (x-y view) of a signal processing technique of a triangular modulated FMCW signal (256 samples, with SNR= 10dB) with threshold value automatically set to 60%. From this threshold plot, the signal was declared a (visual) detection because at least a portion of each of the 4 signal components (the 2 legs for each of the 2 triangles of the triangular modulated FMCW) was visible.

Carrier frequency: The frequency corresponding to the maximum intensity of the time-frequency representation (see Figure 3).

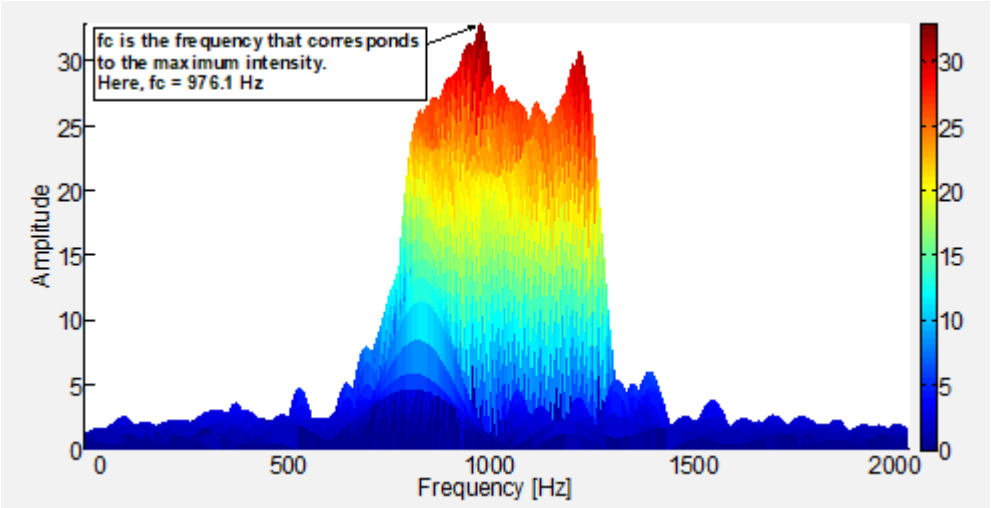

Figure 3: Determination of carrier frequency. Plot of a signal processing technique of a triangular modulated FMCW signal (256 samples, SNR=10dB). From the frequency vs. amplitude (y-z view), the maximum intensity value is manually determined. The frequency corresponding to the max intensity value is the carrier frequency (here fc=976.1Hz).

Modulation bandwidth: Distance from highest frequency value of signal (at a threshold of 20% maximum intensity) to lowest frequency value of signal (at same threshold) in Y-direction (frequency).

The threshold percentage was determined based on manual measurement of the modulation bandwidth of the signal in the time-frequency representation. This was accomplished for ten test runs for each of the signal processing techniques that were used, for the triangular modulated FMCW waveform. During each manual measurement, the max intensity of the high and low measuring points was recorded. The average of the max intensity values for these test runs was 20%. This was adopted as the threshold value, and is representative of what is obtained when performing manual measurements. This 20% threshold was also adapted for determining the modulation period and the time-frequency localization (both are described below).

For modulation bandwidth determination, the 20% threshold value was included for each the signal processing technique algorithms so that the threshold could be applied automatically during the plotting process. From the threshold plot, the modulation bandwidth was manually measured (see Figure 4).

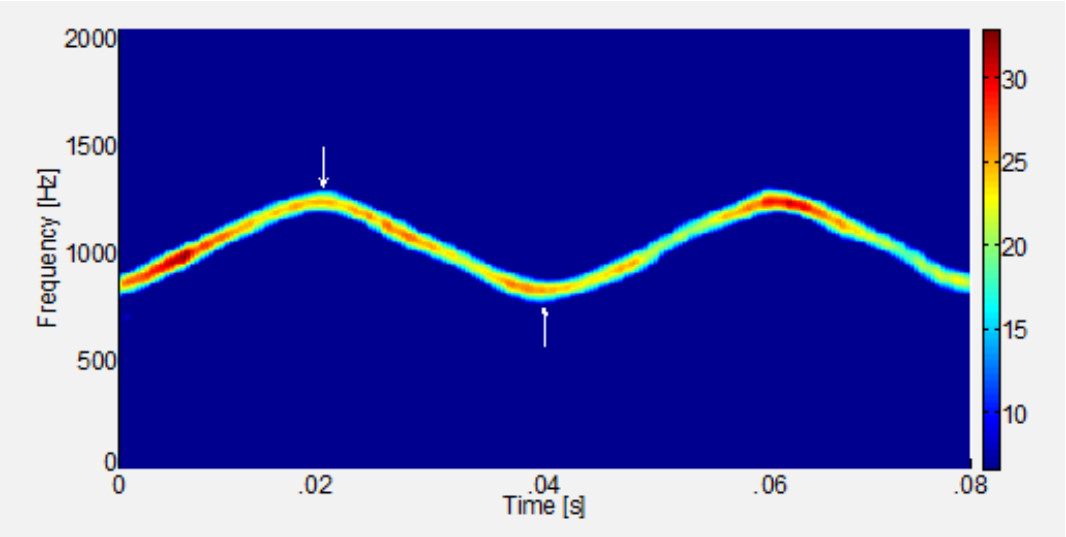

Figure 4: Modulation bandwidth determination. This plot is a time vs. frequency (x-y view) of a signal processing technique of a triangular modulated FMCW signal (256 samples, SNR=10dB) with threshold value automatically set to 20%. From this threshold plot, the modulation bandwidth was measured manually from the highest frequency value of the signal (top white arrow) to the lowest frequency value of the signal (bottom white arrow) in the y-direction (frequency).

Modulation period: Distance from highest frequency value of signal (at a threshold of 20% maximum intensity) to lowest frequency value of signal (at same threshold) in X-direction (time).

For modulation period determination, the 20% threshold value was included for each of the signal processing technique algorithms so that the threshold could be applied automatically during the plotting process. From the threshold plot, the modulation period was manually measured (see Figure 5).

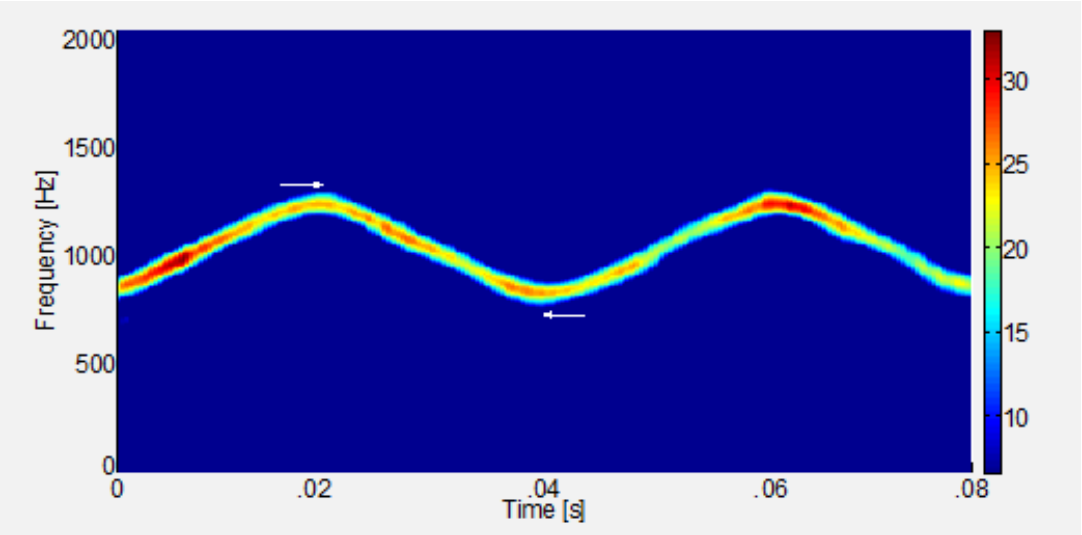

Figure 5: Modulation period determination. This plot is a time vs. frequency (x-y view) of a signal processing technique of a triangular modulated FMCW signal (256 samples, SNR=10dB) with threshold value automatically set to 20%. From this threshold plot, the modulation period was measured manually from the highest frequency value of the signal (top white arrow) to the lowest frequency value of the signal (bottom white arrow) in the x-direction (time).

Time-frequency localization: Measure of the thickness of a signal component (at a threshold of 20% maximum intensity on each side of the component) – converted to % of entire X-Axis, and % of entire Y-Axis.

For time-frequency localization determination, the 20% threshold value was included for each of the signal processing technique algorithms so that the threshold could be applied automatically during the plotting process. From the threshold plot, the time-frequency localization was manually measured (see Figure 6).

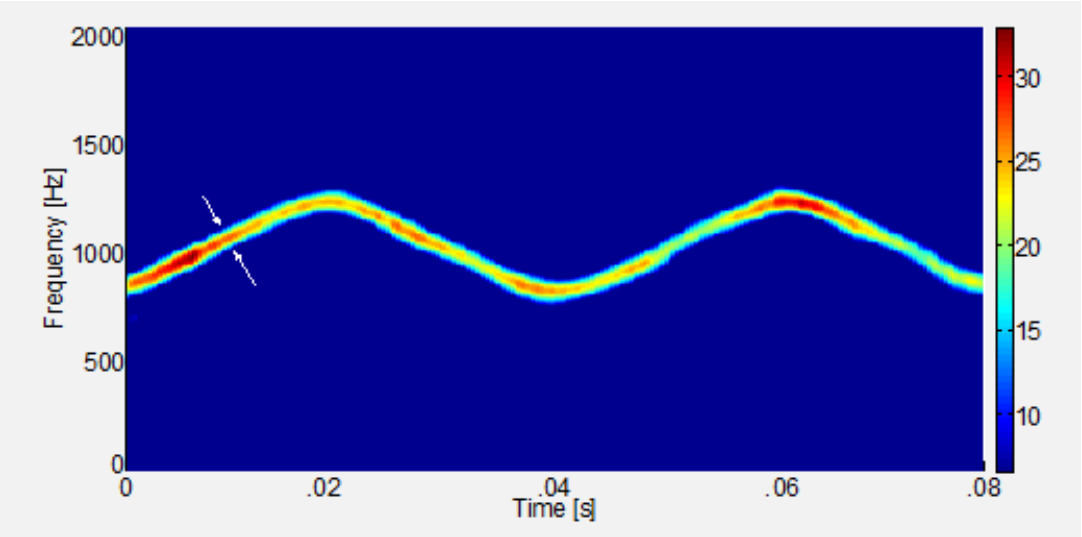

Figure 6: Time-frequency localization determination. This plot is a time vs. frequency (x-y view) of a signal processing technique of a triangular modulated FMCW signal (256 samples, SNR=10dB) with threshold value automatically set to 20%. From this threshold plot, the time-frequency localization was measured manually from the left side of the signal (left white arrow) to the right side of the signal (right white arrow) in both the x-direction (time) and the y-direction (frequency). Measurements were made at the center of each of the 4 'legs', and the average values were determined. Average time and frequency 'thickness' values were then converted to: % of entire x-axis and % of entire y-axis.

Chirp rate: (modulation bandwidth)/(modulation period)

Lowest detectable SNR: The lowest SNR level at which at least a portion of each of the signal components exceeded the set threshold listed in the percent detection section above.

For lowest detectable SNR determination, these threshold values were included for each of the signal processing technique algorithms so that the thresholds could be applied automatically during the plotting process. From the threshold plot, the signal was declared a detection if any portion of each of the signal components was visible. The lowest SNR level for which the signal was declared a detection is the lowest detectable SNR (see Figure 7).

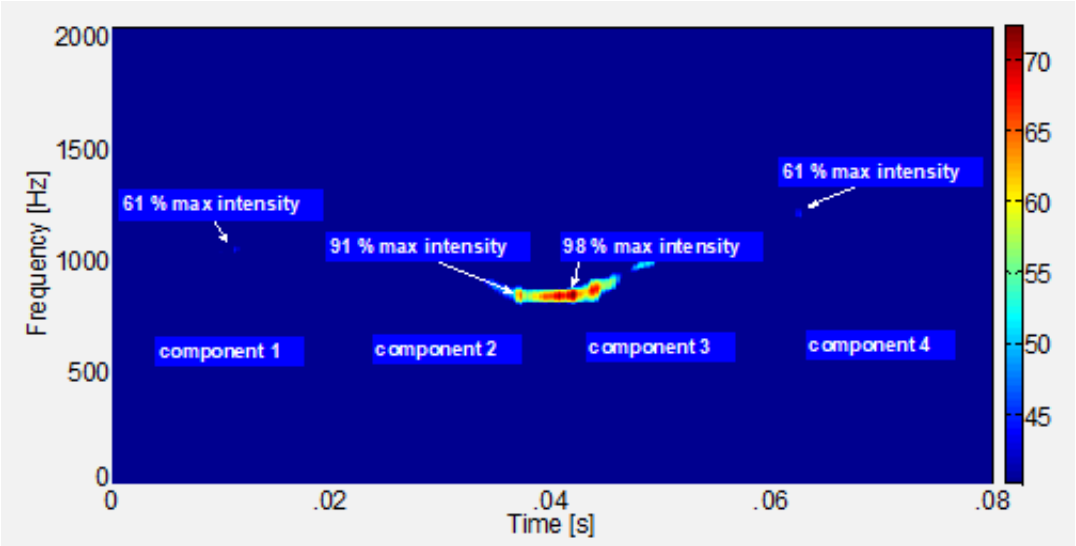

Figure 7: Lowest detectable SNR. This plot is a time vs. frequency (x-y view) of a signal processing technique of a triangular modulated FMCW signal (256 samples, with SNR= -3dB) with threshold value automatically set to 60%. From this threshold plot, the signal was declared a (visual) detection because at least a portion of each of the 4 signal components (the 2 legs for each of the 2 triangles of the triangular modulated FMCW) was visible. Note that the signal portion for the two 61% max intensities are barely visible, because the threshold for this particular signal processing technique is 60%. For this case, any lower SNR than -3dB would have been a non-detect.

The data from all 250 runs for each test was used to produce the actual, error, and percent error for each of the metrics listed above.

The metrics for the WVD signal processing technique were then compared to the metrics for the RSPWVD signal processing technique. By and large, the RSPWVD signal processing technique outperformed the WVD signal processing technique, as will be shown in the results section.

III. Results

Table 1 presents the overall test metrics for the two signal processing techniques used for this testing (RSPWVD versus WVD).

Table 1: Overall test metrics (average percent error: carrier frequency, modulation bandwidth, modulation period, chirp rate; average: percent detection, lowest detectable snr, plot time, time-frequency localization (as a percent of x axis and y axis) for the two signal processing techniques (RSPWVD versus WVD).

Parameters	RSPWVD	WVD
carrier frequency	2.07%	2.46%
modulation bandwidth	3.33%	5.63%
modulation period	2.44%	4.51%
chirp rate	4.57%	7.77%
percent detection	95.6%	74.6%
lowest detectable snr	-3.11db	-2.23db
relative processing time	0.0177s	0.443s
time-frequency localization-x	0.57%	1.68%
time-frequency localization-y	1.64%	4.04%

From Table 1, the RSPWVD outperformed the WVD in average percent error: carrier frequency (2.07% vs. 2.46%), modulation bandwidth (3.33% vs. 5.63%), modulation period (2.44% vs. 4.51%), and chirp rate (4.57% vs. 7.77%). The RSPWVD also outperformed the WVD in average: percent detection (95.6% vs. 74.6%), lowest detectable SNR (-3.11db vs. -2.23db), relative processing time (0.0177s vs. 0.443s), time-frequency localization (x-direction) (0.57% vs. 1.68%), and time-frequency localization (y-direction) (1.64% vs. 4.04%).

Figure 8 shows comparative plots of the RSPWVD (left) vs. the WVD (right) (triangular modulated FMCW signal) at SNRs of 10dB (top row), 0dB (middle row), and lowest detectable SNR (-3dB for RSPWVD and -2dB for WVD) (bottom row).

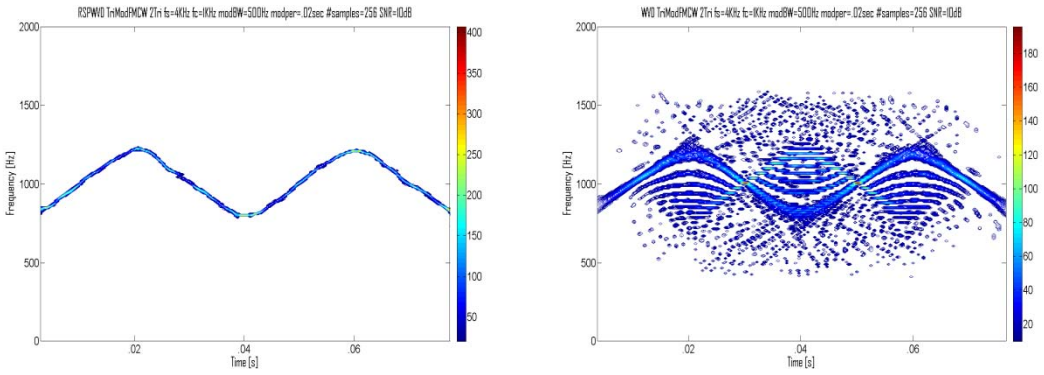

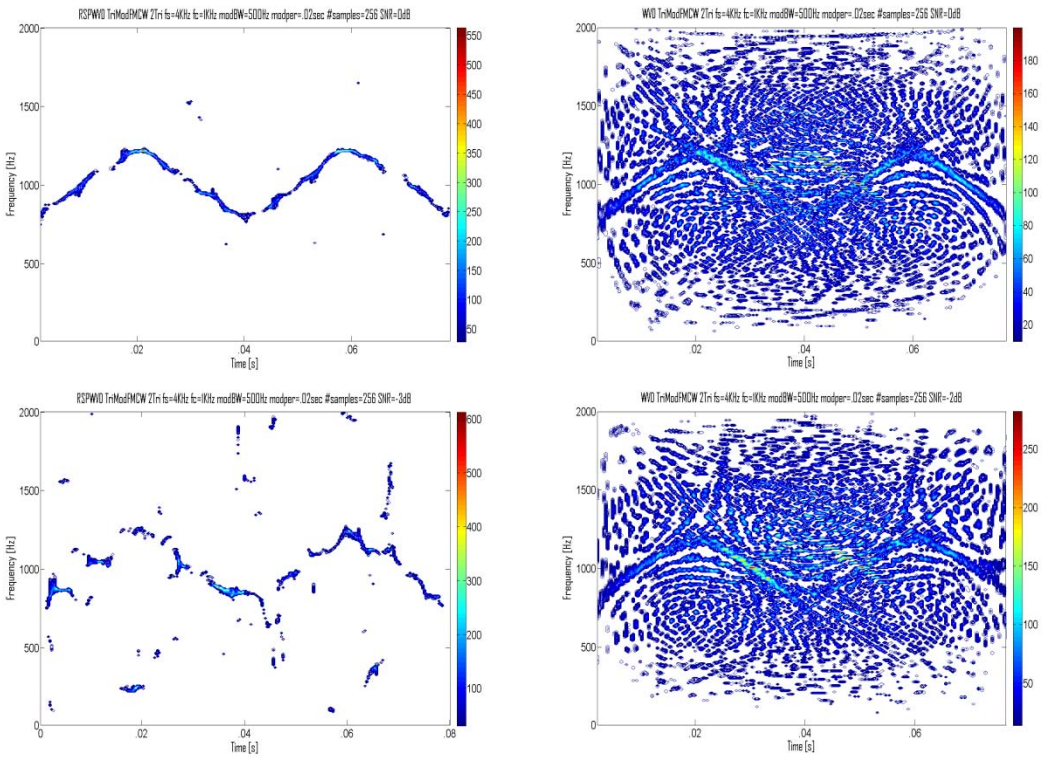

Figure 8: Comparative plots of the triangular modulated FMCW low probability of intercept radar signals (RSPWVD (left-hand side) vs. the WVD (right-hand side)). The SNR for the top row is 10dB, for the middle row is 0dB, and for the bottom row is the lowest detectable SNR(-3dB for RSPWVD; -2 dB for WVD).In general, the RSPWVD signal appears more localized ('thinner') than does the WVD signal, and has no cross-term interference, compared to the WVD.

IV. Discussion

This section will elaborate on the results from the previous section.

From Table 1, the RSPWVD outperformed the WVD in average percent error: carrier frequency (2.07% vs. 2.46%), modulation bandwidth (3.33% vs. 5.63%), modulation period (2.44% vs. 4.51%), and chirp rate (4.57% vs. 7.77%). The RSPWVD also outperformed the WVD in average: percent detection (95.6% vs. 74.6%), lowest detectable SNR (-3.11db vs. -2.23db), relative processing time (0.0177s vs. 0.443s), time-frequency localization (x-direction) (0.57% vs. 1.68%), and time-frequency localization (y-direction) (1.64% vs. 4.04%).

The cross-term interference of the WVD accounts for its: slower relative processing time, lower percent detection, and poorer lowest detectable SNR.

The RSPWVD reduces cross-term interference and has a more localized ('tighter') signal, accounting for its lower average percent error for: carrier frequency, modulation bandwidth, modulation period, and chirp rate – and accounting for its better time-frequency localization (x and y direction).

V. Conclusions

Digital intercept receivers, whose main job is to detect and extract parameters from low probability of intercept radar signals, are currently moving away from Fourier-based analysis and towards classical time-frequency analysis techniques, such as the WVD. Though classical time-frequency analysis techniques are an improvement over Fourier-based analysis techniques, classical time-frequency analysis techniques, in particular the WVD, suffer from cross-term interference, which can make the time-frequency representation hard to read, especially if the components are numerous or close to each other, and the more so in the presence of noise. This lack of readability may equate to less accurate signal detection and parameter extraction metrics, potentially placing the intercept receiver signal analyst's platform in harm's way. This paper examined a potential solution to this problem: the reassignment method, in particular, the RSPWVD signal processing technique, which was found to reduce cross-term interference, making the time-frequency representation much easier to read, leading to more accurate signal detection and parameter extraction metrics. The RSPWVD signal processing technique by-and-large outperformed the WVD signal processing technique in every metrics category. More accurate characterization metrics could well translate into saved equipment and lives.

Future plans include continuing to analyze low probability of intercept radar waveforms (such as the

frequency hopping and the triangular modulated FMCW), using additional signal processing techniques.

References Références Referencias

1. [ANJ09] Anjaneyulu, L., Murthy, N., Sarma, N., A Novel Method for Recognition of Modulation Code of LPI Radar Signals. International Journal of Recent Trends in Engineering, Vol. 1, No. 3, pp. 176-180, May 2009.
2. [AUG94] Auger, F., Flandrin, P., The Why and How of Time-Frequency Reassignment. IEEE International Symposium on Time-Frequency and Time-Scale Analysis, pp. 197-200, 1994.
3. [AUG95] Auger, F., Flandrin, P., Improving the Readability of Time-Frequency and Time-Scale Representations by the Reassignment Method. IEEE Transactions on Signal Processing, 43(5):1068-1089, 1995.
4. [BOA03] Boashash, B., Time Frequency Signal Analysis and Processing: A Comprehensive Reference. Elsevier, Oxford, England, 2003.
5. [GUL07] Gulum, T., Autonomous Non-Linear Classifications of LPI Radar Signal Modulations. Thesis, Naval Postgraduate School, Monterey, CA, 2007.
6. [GUL08] Gulum, T., Pace, P., Cristi, R., Extraction of Polyphase Radar Modulation Parameters Using a Wigner-Ville Distribution-Radon Transform. IEEE International Conference on Acoustics, Speech, and Signal Processing, Las Vegas, NV, April 2008.
7. [HAN00] Han, S., Hong, H., Seo, D., Choi, J., Target Position Extraction Based on Instantaneous Frequency Estimation in a Fixed-Reticle Seeker. Opt. Eng., Vol. 39, pp. 2568-2573, September 2000.
8. [HIP00] Hippenstiel, R., Fargues, M., Moraitakis, I., Williams, C., Detection and Parameter Estimation of Chirped Radar Signals. Final Report, Naval Postgraduate School, Monterey, CA, Jan. 10, 2000.
9. [LIA09] Liang, Y., Zhang, L., Xing, M., Bao, Z., High-Speed Ground Moving Target Detection Research Using Triangular Modulation FMCW. Front. Electr. Electron. Eng., China, 4(2), pp. 127-133, 2009.
10. [LIW08] Li, W., Dan, M., Wang, X., Li, D., Wang, G., Fast Estimation Method and Performance Analysis of Frequency Modulation Rate Via RAT. Proceedings of the 2008 IEEE International Conference on Information and Automation, Zhangjiajie, China, pp. 144-147, June 20-23, 2008.
11. [LIX08] Li, X., Bi, G., A New Reassigned Time-Frequency Representation. 16th European Signal Processing Conference, Lausanne, Switzerland, pp. 1-4, August 25-29, 2008.
12. [LIY03] Li, Y., Xiao, X., Recursive Filtering Radon-Ambiguity Transform Algorithm for Detecting Multi-LFM Signals. Journal of Electronics (China), Vol. 20, No. 3, pp. 161-166, May 2003.
13. [MIL02] Milne, P., Pace, P., Wigner Distribution Detection and Analysis of FMCW and P-4 Polyphase LPI Waveforms. Proceedings of ICASSP, Orlando, FL, pp. 3944-3947, 2002.
14. [OZD03] Ozdemir, A., Time-Frequency Component Analyzer. Dissertation, Bilkent University, Ankara, Turkey, Sept. 2003.
15. [PAC09] Pace, P., Detecting and Classifying Low Probability of Intercept Radar. Artech House, Norwood, MA, 2009.
16. [PAP95] Papandreou, A., Boudreaux-Bartels, G.F., Kay, S., Detection and Estimation of Generalized Chirps Using Time-Frequency Representations. 1994 Conference Record of the Twenty-Eighth Asilomar Conference on Signals, Systems and Computers, pp. 50-54, 1994.
17. [QIA02] Qian, S., Introduction To Time-Frequency and Wavelet Transforms. Prentice Hall, Upper River, NJ, 2002.
18. [RAN01] Rangayyan, R., Krishnan, S., Feature Identification in the Time-Frequency Plane by Using the Hough-Radon Transform. Pattern Recognition, Vol. 34, pp. 1147-1158, 2001.
19. [STE96] Stephens, J., Advances in Signal Processing Technology for Electronic Warfare. IEEE AES Systems Magazine, pp. 31-38, November 1996.
20. [WAJ08] Wang, Y., Jiang, Y., Detection and Parameter Estimation of Multi component LFM Signal Based on the Cubic Phase Function. EURASIP Journal on Advances in Signal Processing, Vol. 2008, Article ID 743985, pp. 1-7, 2008
21. [WAN10] Wang, P., Li, H., Djurovic, I., Himed, B., Integrated Cubic Phase Function for Linear FM Signal Analysis. IEEE Transactions on Aerospace and Electronic Systems, to appear, 2010.
22. [WEI03] Wei, G., Wu, S., Mao, E., Analysis of Multicomponent LFM Signals Using Time-Frequency and The Gray-Scale Inverse Hough Transform. IEEE Workshop on Statistical Signal Processing, pp. 190-193, September 28 – October 1, 2003.
23. [WIL06] Wiley, R., ELINT: The Interception and Analysis of Radar Signals. Artech House, Norwood, MA, 2006.
24. [WON09] Wong, K., Davidson, T., Abelkader, S., Detection of Low Probability of Intercept Radar Signals. Defence R&D Canada – Ottawa Contract Report 2009-142, September 2009.
25. [XIA99] Xia, X., Chen, V., A Quantitative SNR Analysis for the Pseudo Wigner-Ville Distribution. IEEE Transactions on Signal Processing, Vol. 47, No. 10, pp. 2891-2894, October, 1999.